Alternative perspective on quantum tunneling and instantons

F. Paradis,[1] H. Kröger,[1,*] G. Melkonyan,[1] and K. J. M. Moriarty[2]
[1]*Département de Physique, Université Laval, Québec, Québec, Canada G1K 7P4*
[2]*Department of Mathematics, Statistics and Computer Science, Dalhousie University, Halifax, Nova Scotia, Canada B3H 3J5*
(Received 5 August 2004; published 16 February 2005)

We present an alternative way to compute and interpret quantum tunneling in a one-dimensional double-well potential. For large transition time we show that the quantum action functional gives an analytical expression for tunneling amplitudes. This has been confirmed by numerical simulations giving relative errors in the order of 10^{-5}. In contrast to the classical potential, the quantum potential has a triple well if the classical wells are deep enough. Its minima are located at the positions of extrema of the ground state wave function. The striking feature is that a single trajectory with a double instanton reproduces the tunneling amplitude. This is in contrast to the standard instanton approach, where infinitely many instantons and anti-instantons have to be taken into account. The quantum action functional is valid in the deep quantum regime in contrast to the semiclassical regime where the standard instanton approach holds. We compare both approaches via numerical simulations. While the standard instanton picture describes only the transition between potential minima of equal depth, the quantum action may give rise to instantons also for asymmetric potential minima. Such a case is illustrated by an example.

DOI: 10.1103/PhysRevA.71.022106 PACS number(s): 03.65.Xp, 73.43.Jn

I. INTRODUCTION

Tunneling is a characteristic feature of quantum physics, having no counterpart in classical physics. Instantons are known to be intimately connected to tunneling. The physics of instantons and its relation to tunneling have been discussed in Refs. [1,2] and the role of instantons in QCD has been reviewed in Ref. [3]. Tunneling effects and the use of instantons appear in many different areas of physics, such as inflationary scenarios and formation of galaxies [4–7], hot and dense nuclear matter [8], neutrino oscillations [9–11], condensed matter physics [Superconducting quantum interference devices (SQUIDs)] [12,13], quantum computers based on superconductors [14,15], dynamical tunneling [16,17], and chemistry (chemical bindings).

The standard instanton picture is valid in the semiclassical regime. Infinitely many instantons and anti-instantons contribute to give the tunneling amplitude. In this work we consider the opposite regime, i.e., the deep quantum regime. We use the concept of the quantum action, being a kind of effective action, which takes into account quantum effects via tuned action parameters. The action is computed from the ground state of the system. In the limit of large imaginary time, the ground state wave function determines the shape of the quantum potential, which together with a corresponding quantum mass determines the quantum action. The quantum action functional then gives the exact tunneling amplitudes. The shape of the resulting quantum potential is different from the classical double-well potential, i.e., it exhibits a triple-well structure. We find that a double instanton (anti-instanton) is necessary and sufficient to reproduce exactly the tunneling amplitude. The standard instanton approach holds for oscillatorlike potentials with deep wells and high barriers. In contrast to that, the quantum action approach holds when the potential is shallow and the physics is dominated by the ground state properties (Feynman-Kac limit), i.e., in the deep quantum regime. In this sense the quantum action functional is a method complementary to the semiclassical instanton approach.

Another approach in constructing an effective classical potential has been proposed by Feynman and Kleinert [18]. Though similar to the quantum action in its physical goal and motivation, it differs by its definition. When applied to a classical double-well potential [19] it gives an effective potential different from the quantum potential. In particular, the quantum action generates a triple-well potential with degenerate minima (all of equal depth), which is not the case for the effective classical potential.

In Sec. II we present the tunneling model and the construction of the quantum action functional. Section III presents numerical results on how the quantum action functional has been calculated and how well it fits the transition amplitude. In Sec. IV we compare numerical results from the standard instanton approach with those from the quantum action functional. We briefly discuss the use of the quantum action method for asymmetric double-well potentials in Sec. V. Finally, Sec. VI gives a discussion and Sec. VII a summary.

II. MODEL AND ITS QUANTUM ACTION

A. Quantum mechanical tunneling model

Let us consider in one dimension (1D) a classical Hamiltonian system

$$H = \frac{p^2}{2m} + V(x), \tag{1}$$

with a potential of double-well shape given by

*Corresponding author. Email address: hkroger@phy.ulaval.ca

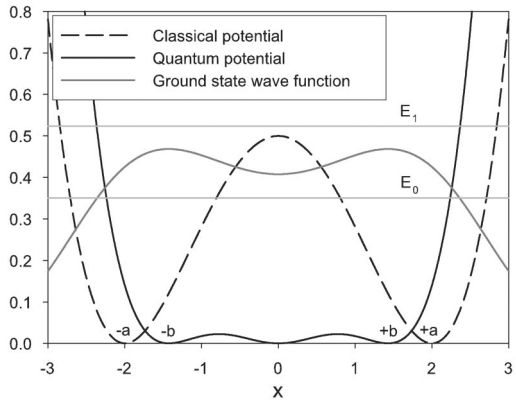

FIG. 1. Classical double-well potential for $\lambda = 1/32$ (minima at $-a$, $+a$), the ground state wave function, and two lowest energy levels. The quantum potential $\tilde{V} - \tilde{V}_0$ (multiplied by a scale factor 1.7331) displays triple wells (minima at $-b$, 0, $+b$). All quantities are in dimensionless units.

$$V(x) \equiv \lambda\left(x^2 - \frac{1}{8\lambda}\right)^2 = \lambda x^4 - \frac{x^2}{4} + \frac{1}{64\lambda}. \tag{2}$$

For simplicity, we use throughout $\hbar = c = m = 1$, which makes all physical units dimensionless. The potential minima are located at $\pm a$, $a = 1/\sqrt{8\lambda}$. A potential barrier of height $B = 1/64\lambda$ is located at $x = 0$ (see Fig. 1). The potential parameters were chosen such that the natural frequency of the oscillations at the bottom of each well is $\omega = 1$ for all λ. The potential is of confinement type, i.e., tends to infinity for large $|x|$. Hence the quantum system has a discrete bound state spectrum (no scattering states) of energies E_n, $n = 0, 1, 2, \ldots$. Depending on the height of the potential barrier B, the following physical situations may occur (i) $B < E_0$. The barrier is lower than the ground state energy. Then the ground state wave function has a single hump at the center. (ii) $E_0 < B$. The ground state energy is lower than the barrier and the ground state wave function displays a double hump. This case is sketched in Fig. 1. (iii) $E_0 < E_1 < \cdots < E_k < B$. The barrier is higher than the first $k+1$ bound state energies. Quantum tunneling in the proper sense occurs in cases (ii) and (iii). The transition between regions (i) and (ii) occurs at $\lambda = 5.345\,813\,36 \times 10^{-2}$. In all plots involving λ, a vertical gray line represents this boundary. The parameter λ controls the barrier height and the property of the system to be located in the semiclassical regime. Large λ means a low barrier (quantum regime) while small λ represents two deep (almost decoupled) wells (semiclassical regime). The tunneling amplitude is given by the (imaginary time) transition matrix element corresponding to the transition from one minimum to the other,

$$\langle a | \exp[-HT/\hbar] | -a \rangle. \tag{3}$$

B. Construction of the quantum action for large transition time

The quantum action has been introduced in Ref. [20]. It is a local action, like the classical action, given by

$$\tilde{S}[x] = \int_0^T dt \frac{\tilde{m}}{2}\dot{x}^2 - \tilde{V}(x), \tag{4}$$

where $\tilde{m}$ is called the quantum mass and $\tilde{V}(x)$ the quantum potential. The quantum action functional is defined as a parametrization of the quantum transition amplitude $G(x_{\rm fi}, t = T; x_{\rm in}, t = 0)$ for arbitrary transition time T in the following way:

$$G(x_{\rm fi}, t = T; x_{\rm in}, t = 0) = \sum_{\text{trajectories}} \tilde{Z} \exp\{i\tilde{S}[\tilde{x}_{\rm traj}]/\hbar\},$$

$$\tilde{x}_{\rm traj} : \delta\tilde{S}[\tilde{x}_{\rm traj}] = 0. \tag{5}$$

Here $\tilde{x}_{\rm traj}$ denotes a trajectory (stationary point) of the action $\tilde{S}$ going from boundary point $(x_{\rm in}, t = 0)$ to $(x_{\rm fi}, t = T)$. There may be several such trajectories.

Tunneling involves imaginary time $(t \to -it)$. Moreover, the instanton picture of tunneling is usually considered in the limit of large transition time $(T \to \infty)$. Hence let us consider from now on time to be imaginary and the transition time T to become large (Feynman-Kac limit). In this limit the quantum action functional has been proven to exist, and to give an exact parametrization of transition amplitudes by taking into account only a single trajectory [21]

$$G_{\rm Eucl}(x_{\rm fi}, t = T; x_{\rm in}, t = 0) \underset{T\to\infty}{\to} \tilde{Z}_{\rm Eucl} \exp\{-\tilde{S}_{\rm Eucl}[\tilde{x}^{\rm traj}_{\rm Eucl}]/\hbar\}, \tag{6}$$

where

$$\tilde{S}_{\rm Eucl}[x] = \int_0^T dt \frac{\tilde{m}}{2}\dot{x}^2 + \tilde{V}(x) \tag{7}$$

denotes the Euclidean action. (Following physics conventions, we dropped the overall minus sign occurring in the action at imaginary time. It will reappear in $\exp[-\tilde{S}_{\rm Eucl}]$.) Here $\tilde{x}^{\rm traj}_{\rm Eucl}$ is the trajectory which makes $\tilde{S}_{\rm Eucl}$ stationary. We use the notation $\tilde{\Sigma} = \tilde{S}[\tilde{x}^{\rm traj}_{\rm Eucl}]$. It should be pointed out that, although being a stationary point of the action $\tilde{S}_{\rm Eucl}$, the trajectory $\tilde{x}^{\rm traj}_{\rm Eucl}$ does not necessarily always minimize the quantum action. Below we will show which particular trajectory must be taken in order to represent the propagator. From now on we drop the subscript "Eucl."

Also in this limit, analytical relations exist between the classical potential, the quantum potential, and wave functions [22]. For example the following relation was established [21]:

$$\frac{2\tilde{m}}{\hbar^2}[\tilde{V}(x) - \tilde{V}_0] = \left(\frac{d\psi_{\rm gr}(x)/dx}{\psi_{\rm gr}(x)}\right)^2 = \left(\frac{d \ln \psi_{\rm gr}(x)}{dx}\right)^2. \tag{8}$$

Here $\tilde{V}_0$ denotes the minimum value of the quantum potential. Those results have been established on the assumption of a nondegenerate ground state and a confining potential with a single minimum. Tunneling involves potentials with multiple (possibly degenerate) minima. Therefore, we take

here Eq. (8) as starting point and aim to construct an expression which generalizes that of Eq. (6)

From the Schrödinger equation one can compute the ground state wave function $\psi_{\rm gr}(x)$ and via Eq. (8) obtain the quantum potential (times the quantum mass). A plot of the quantum potential $\tilde{V}(x)-\tilde{V}_0$ (up to a multiplicative factor) is shown in Fig. 1. The following observations can be made. First, the quantum potential, like the classical potential, is of confining type, i.e., it goes to infinity for large $|x|$. It also displays the same dependence in x^4 for large x. Second, there is a marked difference between the shape of the classical potential and the quantum potential. The former has two wells, but the latter can have one, two, or, in the case shown in Fig. 1, three wells, located at $-b$, 0, and $+b$. Moreover, Eq. (8) shows that $\tilde{V}(x)=\tilde{V}_0$, i.e., the quantum potential reaches a minimum, whenever the ground state wave function has derivative zero, i.e., whenever it reaches a maximum or a minimum. This correspondence between the extrema of the ground state wave function and the quantum action is a property not shared by the classical potential. Finally, the parity symmetry of classical potential is maintained by the quantum potential also.

Integration of Eq. (8) allows us to express the ground state wave function in terms of the quantum mass and potential,

$$\psi_{\rm gr}(x) = Z \exp\left[\pm \int_{x_0}^{x} ds \sqrt{\frac{2\tilde{m}}{\hbar^2}[\tilde{V}(s)-\tilde{V}_0]} \right], \tag{9}$$

where Z is some integration constant. In this section, we will consider only the tunneling regime, where the quantum potential shows a triple-well structure—other cases are simpler. The question arises: Which is the physically valid sign in the exponent? The answer can be found by looking at the shape of $\psi_{\rm gr}(x)$ and $\tilde{V}(x)$. In the regime $-\infty<x<-b$ (regime I), $\psi_{\rm gr}(x)$ decreases when x goes from $-b$ to $-\infty$. In the regime $-b<x<0$ (regime II), $\psi_{\rm gr}(x)$ increases when x goes from zero to $-b$. In the regime $0<x<+b$ (regime III), $\psi_{\rm gr}(x)$ increases when x goes from zero to $+b$. In the regime $+b<x<+\infty$ (regime IV), $\psi_{\rm gr}(x)$ decreases when x goes from $+b$ to $+\infty$. This behavior requires the following choice of signs:

$$\psi_{\rm gr}(x) = \begin{cases} Z_{\rm I} \exp\left[-\int_{x}^{-b} ds \sqrt{(2\tilde{m}/\hbar^2)[\tilde{V}(s)-\tilde{V}_0]} \right], & -\infty < x < -b, \\ Z_{\rm II} \exp\left[+\int_{x}^{0} ds \sqrt{(2\tilde{m}/\hbar^2)[\tilde{V}(s)-\tilde{V}_0]} \right], & -b < x < 0, \\ Z_{\rm III} \exp\left[+\int_{0}^{x} ds \sqrt{(2\tilde{m}/\hbar^2)[\tilde{V}(s)-\tilde{V}_0]} \right], & 0 < x < +b, \\ Z_{\rm IV} \exp\left[-\int_{+b}^{x} ds \sqrt{(2\tilde{m}/\hbar^2)[\tilde{V}(s)-\tilde{V}_0]} \right], & +b < x < \infty. \end{cases} \tag{10}$$

At the boundary of the regimes, the wave function has to be continuous. This implies relations between the factors $Z_{\rm I},\ldots,Z_{\rm IV}$,

$$\psi_{\rm gr}^{\rm I}(-b) = \psi_{\rm gr}^{\rm II}(-b) \Rightarrow Z_{\rm I} = Z_{\rm II} \exp\left[+\int_{-b}^{0} ds \sqrt{(2\tilde{m}/\hbar^2)[\tilde{V}(s)-\tilde{V}_0]} \right], \quad x=-b,$$

$$\psi_{\rm gr}^{\rm II}(0) = \psi_{\rm gr}^{\rm III}(0) \Rightarrow Z_{\rm II} = Z_{\rm III}, \quad x=0,$$

$$\psi_{\rm gr}^{\rm III}(+b) = \psi_{\rm gr}^{\rm IV}(+b) \Rightarrow Z_{\rm III} \exp\left[+\int_{0}^{+b} ds \sqrt{(2\tilde{m}/\hbar^2)[\tilde{V}(s)-\tilde{V}_0]} \right] = Z_{\rm IV}, \quad x=+b.$$

Because the ground state wave function $\psi_{\rm gr}(x)$ and the quantum potential Eq. (8) are parity symmetric, the previous equations reduce to

$$Z_{\rm II} = Z_{\rm III} \equiv Z,$$

$$Z_{\rm I} = Z_{\rm IV} = ZJ,$$

$$J \equiv \exp\left[+\int_{0}^{+b} ds \sqrt{\frac{2\tilde{m}}{\hbar^2}[\tilde{V}(s)-\tilde{V}_0]} \right]. \tag{11}$$

Z is a factor which normalizes the wave function to unity, and $\log J$ will turn out to be the quantum action of the quantum instanton.

Taking into account those continuity conditions Eq. (11), the wave function $\psi_{\rm gr}(x)$ can be expressed as

$$\psi_{\rm gr}(x) = Z\begin{cases} \exp\left[-\int_x^{-b} ds\sqrt{(2\tilde{m}/\hbar^2)[\tilde{V}(s)-\tilde{V}_0]}+\int_{-b}^{0} ds\sqrt{(2\tilde{m}/\hbar^2)[\tilde{V}(s)-\tilde{V}_0]}\right], & -\infty < x < -b, \\ \exp\left[+\int_x^{0} ds\sqrt{(2\tilde{m}/\hbar^2)[\tilde{V}(s)-\tilde{V}_0]}\right], & -b < x < 0, \\ \exp\left[+\int_0^{x} ds\sqrt{(2\tilde{m}/\hbar^2)[\tilde{V}(s)-\tilde{V}_0]}\right], & 0 < x < +b, \\ \exp\left[+\int_0^{+b} ds\sqrt{(2\tilde{m}/\hbar^2)[\tilde{V}(s)-\tilde{V}_0]}-\int_{+b}^{x} ds\sqrt{(2\tilde{m}/\hbar^2)[\tilde{V}(s)-\tilde{V}_0]}\right], & +b < x < +\infty. \end{cases} \tag{12}$$

The terms occurring in the exponents are related to the quantum action. Because the action is derived from a potential, energy is conserved. In imaginary time it reads

$$E = -\tilde{T} + \tilde{V} = \text{const}, \tag{13}$$

where $\tilde{T} = \frac{1}{2}\tilde{m}\dot{\tilde{x}}_{\rm tr}^2$ denotes the kinetic term. Thus Eq. (13) can be resolved for the velocity,

$$\dot{\tilde{x}}_{\rm tr} = \pm\sqrt{\frac{2}{\tilde{m}}[\tilde{V}(\tilde{x}_{\rm tr})-E]}. \tag{14}$$

Then we can express the quantum action,

$$\begin{aligned} \tilde{\Sigma}_{x_{\rm in},0}^{x_{\rm fi},T} &= \int_0^T dt\,\tilde{T}+\tilde{V} \\ &= \int_0^T E + 2\tilde{T} \\ &= ET + \int_0^T dt\,\tilde{m}\dot{\tilde{x}}_{\rm tr}^2 \\ &= ET + \int_{x_{\rm in}}^{x_{\rm fi}} d\tilde{x}\,\tilde{m}\dot{\tilde{x}}_{\rm tr} \\ &= ET + \int_{x_{\rm in}}^{x_{\rm fi}} dx \pm \sqrt{2\tilde{m}[\tilde{V}(x)-E]}, \end{aligned} \tag{15}$$

where the sign is determined by the sign of the velocity $\dot{\tilde{x}}_{\rm tr}$.

Now we consider the quantum mechanical transition amplitude in imaginary time in the limit $T\to\infty$ (Feynman-Kac limit),

$$G(y,T{:}x,0) \underset{T\to\infty}{\sim} \psi_{\rm gr}(y)\exp[-E_{\rm gr}T/\hbar]\psi_{\rm gr}(x). \tag{16}$$

The coordinates x,y may be located in any of the regimes I,II,III,IV. For example, let us consider $x,y\in I(-\infty<x,y<-b)$. Combining Eqs. (16) and (12) yields

$$\begin{aligned} G(y,T{:}x,0) = Z^2 \exp[-E_{\rm gr}T/\hbar] &\times \exp\left[-\int_0^{-b} ds\sqrt{\frac{2\tilde{m}}{\hbar^2}[\tilde{V}(s)-\tilde{V}_0]}\right. \\ &\left.+\int_{-b}^{y} ds\sqrt{\frac{2\tilde{m}}{\hbar^2}[\tilde{V}(s)-\tilde{V}_0]}\right] \\ &\times \exp\left[-\int_x^{-b} ds\sqrt{\frac{2\tilde{m}}{\hbar^2}[\tilde{V}(s)-\tilde{V}_0]}\right. \\ &\left.+\int_{-b}^{0} ds\sqrt{\frac{2\tilde{m}}{\hbar^2}[\tilde{V}(s)-\tilde{V}_0]}\right]. \end{aligned} \tag{17}$$

There are five contributions in the exponent. Each of them can be identified with the quantum action of some trajectory. For example, consider the term

$$\exp\left[-\int_x^{-b} ds\sqrt{\frac{2\tilde{m}}{\hbar^2}[\tilde{V}(s)-\tilde{V}_0]}\right]. \tag{18}$$

It corresponds to a trajectory starting from x and approaching $-b$ some time later, i.e., entering the valley of the quantum potential at $-b$ (see Fig. 2). Because the velocity $\dot{x}>0$ along the trajectory, the corresponding sign in the quantum action is $+$. Thus the quantum action is

$$\tilde{\Sigma}_x^{-b} = +\int_x^{-b} ds\sqrt{2\tilde{m}[\tilde{V}(s)-\tilde{V}_0]}. \tag{19}$$

The term occurring in G is

$$\exp\left[-\int_x^{-b} ds\sqrt{\frac{2\tilde{m}}{\hbar^2}[\tilde{V}(s)-\tilde{V}_0]}\right] = \exp\left[-\frac{1}{\hbar}\tilde{\Sigma}_x^{-b}\right], \tag{20}$$

which is valid, when we identify $E=\tilde{V}_0$. It gives a minus sign in front of the action. Similarly, the other contributions to G can be expressed as some part of the trajectory shown in Fig. 2. The term

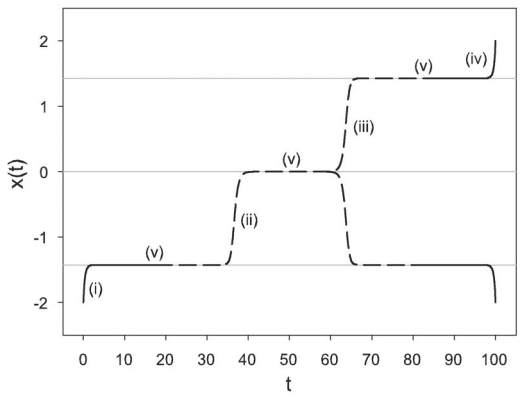

FIG. 2. Trajectory derived from quantum action $\tilde{\Sigma}$ for boundary conditions $x_{\mathrm{in}}=-2$ and $x_{\mathrm{fi}}=\pm 2$ ($\lambda=1/32$ and $T=100$). Full line $\exp[-\tilde{\Sigma}]$. Dashed line $\exp[+\tilde{\Sigma}]$. Minima of quantum potential are indicated by thin gray lines. All quantities are in dimensionless units.

$$\exp[-E_{\mathrm{gr}}T/\hbar] \tag{21}$$

corresponds to the trajectory, where the particle rests either in the valley at $-b$ or in the valley at 0 (having identified $E_{\mathrm{gr}}=\tilde{V}_0$).

To sum up, in the quantum mechanical transition amplitude occur contributions from five different trajectories. They are the trajectory from x to $-b$, then a straight-line trajectory in the valley at $-b$, then a trajectory going over from the valley at $-b$ to the valley at 0, then a straight-line trajectory in the valley 0, then a trajectory going over from the valley 0 to the valley $-b$, then a straight-line trajectory in the valley 0, and finally the trajectory going from the valley $-b$ to the final boundary point y. The transition amplitude then becomes

$$G(y,T;x,0)=Z^2\exp\left[\frac{1}{\hbar}\{-\tilde{\Sigma}_x^{-b}+\tilde{\Sigma}_{-b}^{0}+\tilde{\Sigma}_0^{-b}-\tilde{\Sigma}_{-b}^{y}-\tilde{\Sigma}_{\mathrm{Sl}}\}\right]. \tag{22}$$

Note that the straight-line trajectory contribution can be taken out of the action integral by computing the action in the potential $\tilde{V}-\tilde{V}_0$ and adding $-E_{\mathrm{gr}}T/\hbar$ to the action afterward. The full trajectory is shown in Fig. 2. The full line corresponds to those parts of the trajectory corresponding to the minus sign, while the dashed line corresponds to parts with the plus sign. Let us take a closer look at the trajectories shown in Fig. 2. The trajectory going from $x=-2$ at $t=0$ to $x=-2$ at $t=100$ has a contribution from an instanton and an anti-instanton. Note that this trajectory does not minimize the quantum action due to the contribution of the instanton–anti-instanton pair. This contribution is necessary to correctly normalize the propagator. Other trajectories (corresponding to other initial and final points) are built in the same way. If we assign to each piece of trajectory a corresponding sign in front of the quantum action, we can write

$$G(y,T;x,0)=Z^2\exp\left[\frac{1}{\hbar}\sum_{\mathrm{traj}(\nu)}\mathrm{sgn}_{\mathrm{traj}(\nu)}\tilde{\Sigma}_{\mathrm{traj}(\nu)}\right]. \tag{23}$$

For other regimes, where the quantum potential has only one well, the correct trajectory is much simpler to find and all of it is accounted negatively in the action.

III. NUMERICAL SIMULATIONS

In this section we want to present numerical simulations of the quantum action and see how well it fits the transition amplitudes. The computation of the quantum action functional requires us to compute a trajectory. Such a trajectory is a solution of the Euler-Lagrange equation of motion (in imaginary time), and satisfies boundary conditions at initial and final points. The numerical solution of such differential equations has been found to be most convenient and give stable results by using a relaxation algorithm. To give an example how we have proceeded, consider Fig. 2, in particular, the trajectory going from $x=-2$ to $+2$. Let us recall that we work in the regime where the transition time T is large. In this regime we observe that the trajectory has three pieces, where its motion follows the bottom of a potential valley (first from $t=5$ to 35, second from $t=45$ to 60, finally from $t=70$ to 95). Each of those pieces of trajectory in the valley can be cut somewhere in the middle. As a result the whole trajectory is decomposed into four parts; first from $t=0$ to 20, second from $t=20$ to 50, third from $t=50$ to 80, and fourth from $t=80$ to 100. Each of those four pieces can be computed separately in a numerical way. Finally, the assignment of the sign of the quantum action is taken from the above theoretical analysis.

The system provides two quantities that can be used to find a characteristic time scale, namely, the natural frequency of oscillation in each well ($T_{\mathrm{scale}}^{(1)}=\omega^{-1}=1$) and the ground state energy of the system ($T_{\mathrm{scale}}^{(2)}=\hbar/E_{\mathrm{gr}}$). Since E_{gr} is in the order of 1 in the range of parameters considered in this paper (and since we work in units where $\hbar=1$), we simply take $T_{\mathrm{scale}}=1$. We chose to study transitions at times $T=10$ and 100, which are both large compared to the dynamical time scale. For large transition times $T\gg T_{\mathrm{scale}}$ the transition amplitude is dominated by the ground state and a few excited states. The wave functions and energies of those states have been computed by numerically solving the Schrödinger equation. The quantum action Eq. (4) is determined by the parameter of the quantum mass $\tilde{m}$ and the quantum potential $\tilde{V}(x)$. We computed the function $\tilde{m}[\tilde{V}(x)-\tilde{V}_0]$ from Eq. (8). In order to determine the quantum mass we need another equation. In the Feynman-Kac limit, one cannot directly find the quantum mass independently from the quantum potential. The physical reason is that in the Feynman-Kac limit physics is dominated by the ground state. According to Eq. (9), in the ground state wave function occurs the product of quantum mass and quantum potential. The mathematical reason is that there is a symmetry transformation [21], which keeps the transition amplitude and the quantum action invariant. The transformation

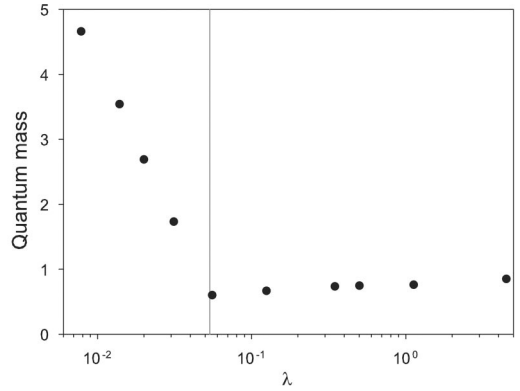

FIG. 3. Quantum mass vs parameter λ. $T=10$. All quantities are in dimensionless units.

$$m \to m' = m/\alpha,$$

$$V(x) \to V'(x) = \alpha V(x),$$

$$T \to T' = T/\alpha \tag{24}$$

leaves the transition amplitudes $G(y,T;x,0)$ invariant. The transformation

$$\tilde{m} \to \tilde{m}' = \tilde{m}/\alpha,$$

$$\tilde{V}(x) \to \tilde{V}'(x) = \alpha \tilde{V}(x),$$

$$T \to T' = T/\alpha \tag{25}$$

leaves the quantum action $\tilde{\Sigma}^{y,T}_{x,0}$ invariant. This invariance implies that the choice of the quantum mass $\tilde{m}$ is arbitrary when T is very large: this symmetry strictly holds in the limit $T \to \infty$. Numerically, we found that this freedom in the choice of $\tilde{m}$ was valid to good precision for $T \geqslant 100$, that is, the value of the quantum mass had no significant influence on the transition amplitudes for $T=100$. However, this was found not to be the case for $T=10$. Therefore, we need additional information about the system to find the correct quantum mass for $T=10$. We have proceeded in the following way. For a given value of λ we made an initial guess of the quantum mass $\tilde{m}$. Then we computed the quantum action for a number of initial points x_{in} and final points x_{fi}, taken from a set $\{x_1,\ldots,x_N\}$. Thus we generated a matrix of quantum action elements Σ^j_i. Via the quantum action functional $G_{ij} = Z \exp[\Sigma^j_i]$, we computed a matrix of transition matrix elements. Diagonalization of G_{ij} yields eigenvalues $E_n T/\hbar$. Then we made a variational search in the parameter $\tilde{m}$, until the energy of the first excited state E_1 obtained from diagonalization of G_{ij} agreed with the exact value (obtained from the solution of the Schrödinger equation). On the other hand, previous numerical experiments have shown that the quantum mass (and also the parameters of the quantum potential) asymptotically converge when $T \to \infty$. Therefore, we simply chose the same values of the quantum mass in the $T=100$ case. The obtained results for the quantum mass are shown in Fig. 3 as a function of the parameter λ. One observes for large $\lambda(\lambda > 6\times 10^{-2})$ a smooth behavior of $\tilde{m}$. At $\lambda \approx 5.3 \times 10^{-2}$ there is a cusp. In our opinion the behavior for $\lambda < 5\times 10^{-2}$ is unphysical, caused by limited numerical precision and the fact that in this regime the contribution to the propagator from the first excited state becomes nonnegligible. However, this uncertainty does not translate into a large error on the transition amplitudes because of their vanishing dependence on the quantum mass in the limit $T \to \infty$. The relative error of the transition amplitude as a function of final position y, while keeping the initial position fixed ($x=0$), is shown in Fig. 4 for $T=100$ and $\lambda = \frac{1}{32}$. The error is larger for large y because the numerical error on the quantum potential is larger for large $|x|$.

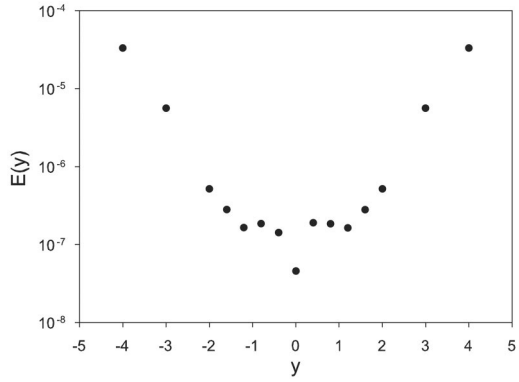

FIG. 4. Relative error $E(y) = |[G(y,T:0,0)_{QA} - G(y,T:0,0)_{\text{Schrod}}]/G(y,T:0,0)_{\text{Schrod}}|$ of transition amplitude for various final positions y for $T=100$ and $\lambda = 1/32$. All quantities are in dimensionless units.

IV. TUNNELING: COMPARISON WITH INSTANTON PICTURE

We have determined the tunneling amplitude

$$G_{Tun} \equiv G(a,T;-a,0) = \langle a|\exp[-HT/\hbar]|-a\rangle, \tag{26}$$

where $\pm a$ are the minima of the classical potential, for various values of the potential parameter λ and transition time T. As reference value, the tunneling amplitude has been computed by solving the Schrödinger equation. Next, the tunneling transition amplitude has been computed from the quantum action functional, that is, by computing the quantum potential and the quantum mass for each of the different classical potentials and transition times and by using the tools developed in Sec. II. Moreover, the transition amplitudes have been obtained by using the semiclassical multiinstanton expression at two-loop order, given by Ref. [3],

$$G_{\text{tun}} = \sqrt{\frac{\omega}{\pi}}\left(1+\frac{3}{8S_0}\right)\exp\left(-\frac{\omega T}{2}\left[1-\frac{1}{3S_0}\right]\right) \times \sinh\left(\sqrt{\frac{6S_0}{\pi}}\exp\left[-S_0-\frac{71}{72}\frac{1}{S_0}\right]\omega T\right), \tag{27}$$

where $\hbar=1$ and $S_0 \equiv 1/(12\lambda)$ is the action of the instanton between classical minima. Results are shown in Figs. 5 and 6 for $T=10$ and 100, respectively. The relative difference be-

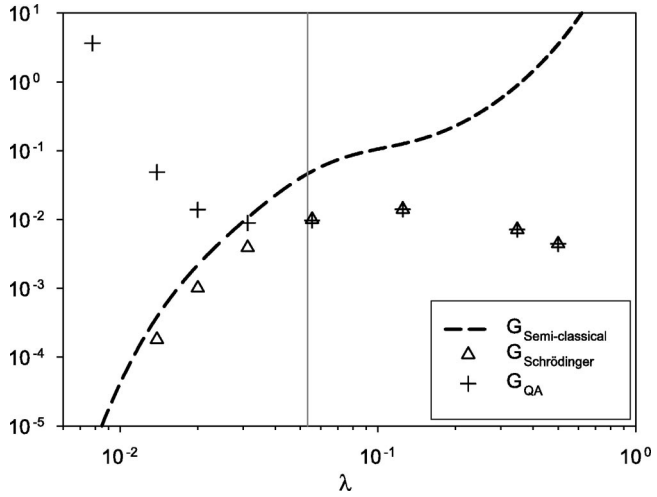

FIG. 5. Tunneling amplitude $G(a,T;-a,0)$ vs potential parameter λ. $T=10$. Comparison of exact result (from the Schrödinger equation) with result from quantum action functional and from instanton method (semiclassical). All quantities are in dimensionless units.

tween the exact tunneling amplitude (from the Schrödinger equation) and the quantum action amplitude for $T=10$ and 100 is shown in Fig. 7. The instanton method is valid in the semiclassical limit where the action S_0 of the classical instanton is large compared to unity (corresponding to small λ). This is clearly the case in Figs. 5 and 6 where the semiclassical tunneling amplitude is quite close to the exact amplitude for small λ. In contrast, the tunneling amplitude computed from the quantum action is better at large λ. It diverges substantially from the exact result for small λ. This divergence is *not* due to a bad choice of quantum mass. It can rather be explained by the fact that the quantum action is constructed from the exact propagator *in the Feynman-Kac limit*, where only the ground state contributes to the physics of the system. However, when λ decreases, the wells get deeper and the energy of the first excited approaches the ground state energy. Then the first excited state contribution

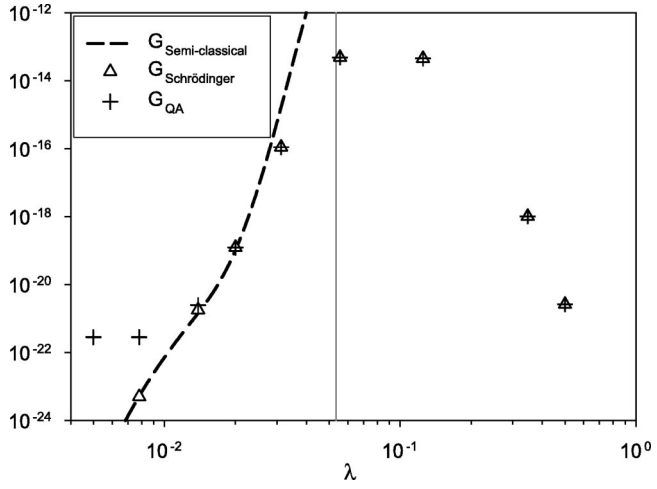

FIG. 6. Same as Fig. 5 but $T=100$. All quantities are in dimensionless units.

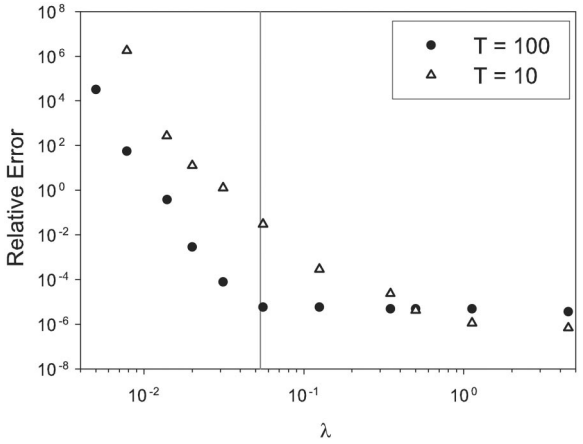

FIG. 7. Relative error of the tunneling amplitude from the quantum action functional with respect to exact result, for $T=10$ and 100. All quantities are in dimensionless units.

cannot be neglected anymore (the ground state becomes degenerate). We can verify that the quantum action functional indeed reproduces correctly the ground state contribution to the propagator $|\psi_{\rm gr}\rangle e^{-E_{\rm gr}T/\hbar}\langle\psi_{\rm gr}|$ for all λ, up to numerical limits. The relative error of tunneling amplitudes from the quantum action is shown in Fig. 7. The fact that the error is generally higher for $T=10$ confirms this observation (lower transition time means that the first excited state is more important in the transition amplitude for the same value of λ). It turns out that the quantum action can be used to compute transition amplitudes for a wide range of potential parameters.

V. TUNNELING IN ASYMMETRIC POTENTIALS

Another advantage of the quantum action functional is that it can be used to study tunneling in an asymmetric double-well potential, with wells of different depth. While such a system is much harder to study in the standard instanton picture, it does not require substantially more work in the quantum action context. In fact, the quantum potential will still display one, two, or three minima, *having all the same depth*. Instanton trajectories similar to those in the standard double-well case then appear likewise. For example, consider the potential

$$V(x)=\frac{1}{50}\left[x^2-\left(\frac{5}{2}\right)^2\right]^2+\frac{1}{250}\left[x-\frac{5}{2}\right]^2, \qquad (28)$$

which is shown in Fig. 8. This potential has two wells, but the left well is higher than the right one, and therefore a classical instanton does not exist. The quantum potential (up to a multiplicative factor) recovered from the ground state wave function is also shown in Fig. 8. We find that the quantum mass in this case (for $T=100$) is about $\tilde{m}=0.11$ and that the tunneling transition amplitude $G(a,T;-a,0)$ reproduces the exact value with a relative error of 2.87×10^{-4}.

VI. DISCUSSION

Using the quantum action functional to describe tunneling in a double-well potential gives good results in the deep

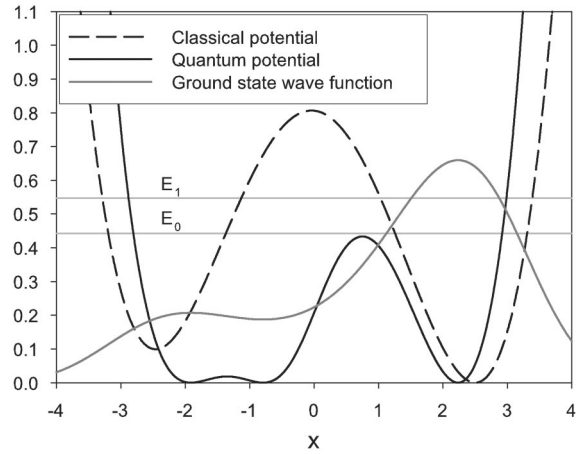

FIG. 8. Asymmetric double-well potential Eq. (28), the ground state wave function, and corresponding quantum potential $\tilde{V}-\tilde{V}_0$ (up to a multiplicative factor). All quantities are in dimensionless units.

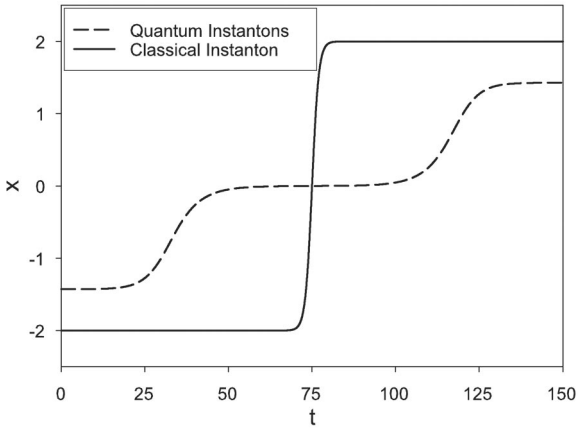

FIG. 9. Comparison between the classical and quantum instantons, for $\lambda = 1/32$. All quantities are in dimensionless units.

quantum regime (opposite to the semiclassical regime). Quantum effects appear in the quantum action via tuned parameters. In the case of tunneling in a classical double-well potential this leads to a quantum potential with a different well structure, having possibly one, two, or three wells. As in the standard instanton picture, quantum instantons occur also in the tunneling amplitude obtained by the quantum action functional. Instantons play an important role in many domains of physics so one may ask how important are the instantons in this case. First, we saw that they play a normalization role in the trajectories, that is, they ensure that the propagator is correctly normalized. Second, as much as standard instantons represent the only finite action solution (in the limit $T\to\infty$) contributing to the propagator between the classical minima, we can interpret the additional instantons as the only finite action solutions (in the $T\to\infty$ limit) contributing to the propagator *between the minima of the quantum potential*. Because these minima of the quantum potential correspond in position to the extrema of the ground state wave function, the double quantum instanton going from $-b$ to 0 to b represents the trajectory reproducing the largest transition amplitude. In particular, the tunneling amplitude between the minima of the quantum potential $\langle -b|\exp[-HT/\hbar]|b\rangle$ is larger than the tunneling amplitude between the minima of the classical potential $\langle -a|\exp[-HT/\hbar]|a\rangle$. Third, one might wonder why in the quantum action functional only two instantons (anti-instantons) contribute, while in the standard approach infinitely many instantons and anti-instantons are needed. The answer is simply that the quantum action was explicitly constructed to reproduce *exactly*, in the Feynman-Kac limit, the transition amplitude, using a single trajectory. This is sufficient to discard the use of multiple instanton trajectories. Fourth, let us compare the structure of the classical instanton with the quantum instanton. The instanton solution corresponding to the classical Hamiltonian of Eqs. (1) and (2), is given by

$$x_{\mathrm{inst}}(t) = \frac{1}{\sqrt{8\lambda}}\tanh\left[\frac{1}{\sqrt{4m}}(t-t_c)\right] = \sqrt{8B}\tanh\left[\frac{1}{\sqrt{4m}}(t-t_c)\right], \tag{29}$$

where B denotes the barrier height of the potential and t_c is the center of the instanton. The steepness of the instanton at its center is given by

$$\frac{d}{dt}x_{\mathrm{inst}}(t=t_c) = \sqrt{\frac{2B}{m}}. \tag{30}$$

Figure 1 shows that that the barrier height of the quantum potential is much smaller than that of the classical potential. The quantum mass is of the same order of magnitude as the classical mass. From Eq. (30) we expect that the steepness of the quantum instanton is smaller than that of the classical instanton. This is confirmed by a numerical calculation, comparing the classical with the quantum instanton, shown in Fig. 9. Also, because the locations of the potential minima are closer for the quantum potential than for the classical potential, the quantum instanton has a smaller action than the classical one. The bottom line is that the quantum instanton is "softer" than the classical instanton. It is interesting to note that a similar observation has been made previously in the context of comparing classical chaos with quantum chaos, again using the quantum action functional [23]. It has been found that the quantum action yields a less chaotic phase space than the classical action. The underlying reason for such behavior is unknown to us. We believe that a promising strategy may be to analyze the path integral and its relation to the quantum action functional.

VII. SUMMARY

This work is about tunneling described in terms of the quantum action functional. This point of view is complementary to the standard instanton picture: While the latter holds in the semiclassical regime, the former holds in the deep quantum regime. The observation that the quantum potential has additional minima (in number and location) beyond those of the classical potential may be of interest for cosmol-

ogy and inflationary models. There are experiments on tunneling in condensed matter, e.g., Josephson junctions, SQUIDS [12,13], or in atomic physics in dynamical tunneling of atoms in a time-dependent exterior field [16,17]. It would be interesting to explore if the quantum action functional can be applied to describe such physics. This requires further development, in particular, to explore the quantum action functional in real time and for explicitly time-dependent systems. Likewise one may ask if tunneling out of metastable states can be described in our approach. We have shown that an asymmetric double-well potential which may give rise to metastable states (which occur, e.g., in nuclear fission and emission of α particles) can be treated in this framework, provided that the potential is bounded from below (which excludes a potential like $V \sim x^3$). However, the description of tunneling from quasistationary states to the ground state or other excited states would require to apply the quantum action in real time. This will be a subject of further studies.

ACKNOWLEDGMENTS

F.P., H.K., and K.M. have been supported by NSERC Canada. H.K. is very grateful to E. Shuryak and T. Schäfer for discussions.

[1] S. Coleman, *Aspects of Symmetry* (Cambridge University Press, Cambridge, U.K., 1985), p. 265.
[2] R. Rajaraman, *Solitons and Instantons* (Elsevier, Amsterdam, 1982).
[3] T. Schäfer and E. V. Shuryak, Rev. Mod. Phys. **70**, 323 (1998).
[4] A. Starobinsky, JETP Lett. **30**, 682 (1979); Phys. Lett. **91B**, 99 (1980).
[5] M. Y. Khlopov, *Cosmoparticle Physics* (World Scientific, Singapore, 1998).
[6] E. W. Kolb, Phys. Scr. **36**, 199 (1991).
[7] H. Jirari, H. Kröger, X. Q. Luo, K. J. M. Moriarty, and S. G. Rubin, Phys. Lett. A **281**, 1 (2001).
[8] E. V. Shuryak, *The QCD Vacuum, Hadrons and Superdense Matter* (World Scientific, Singapore, 1988); Nucl. Phys. B (Proc. Suppl.) **83-84**, 103 (2000).
[9] S. Pastor and G. Raffelt, Phys. Rev. Lett. **89**, 191101 (2002).
[10] C. J. Horowitz and Gang Li, Phys. Rev. Lett. **82**, 5198 (1999).
[11] M. Lindner, e-print hep-ph/0210377.
[12] J. R. Friedman, V. Patel, W. Chen, S. K. Toipygo, and J. E. Lukens, Nature (London) **406**, 43 (2000).
[13] D. V. Averin, J. R. Friedman, and J. E. Lukens, e-print cond-mat/0005081.
[14] A. M. Gulian and K. S. Wood, e-print quant-ph/0207098 (to be published).
[15] A. M. Gulian and K. S. Wood, e-print cond-mat/0207424.
[16] D. A. Steck, W. H. Oskay, and M. G. Raizen, Science **293**, 274 (2001).
[17] W. K. Hensinger, H. Häffner, A. Browaeys, N. R. Heckenberg, K. Helmerson, C. McKenzie, G. J. Wilburn, W. D. Phillips, S. L. Roiston, H. Rubinsztein-Dunlop, and B. Upcroft, Nature (London) **412**, 52 (2001).
[18] R. P. Feynman and H. Kleinert, Phys. Rev. A **34**, 5080 (1986).
[19] W. Janke and H. Kleinert, Chem. Phys. Lett. **137**, 162 (1987).
[20] H. Jirari, H. Kröger, X. Q. Luo, K. J. M. Moriarty, and S. G. Rubin, Phys. Rev. Lett. **86**, 187 (2001).
[21] H. Kröger, Phys. Rev. A **65**, 052118 (2002).
[22] H. Jirari, H. Kröger, X. Q. Luo, G. Melkonyan, and K. J. M. Moriarty, Phys. Lett. A **303**, 299 (2002).
[23] L. A. Caron, D. Huard, H. Kröger, G. Melkonyan, K. J. M. Moriarty, and L. P. Nadeau, Phys. Lett. A **322**, 60 (2004).